Original Article

A novel nebulized drug delivery system based on an innovative high-pressure peristaltic pump availably applied to pressurized intraperitoneal aerosol chemotherapy

Renjie Li[1,2,3#], Qiming Fan[2#], Xiaosong Lin[2,4#], Ruijian Chen[2,5], Bingcong Luo[2,6], Zifeng Yang[2], Yong Li[1,2]

[1]Guangdong Cardiovascular Institute, Guangdong Provincial People's Hospital, Guangdong Academy of Medical Sciences, Guangzhou, China; [2]Department of Gastrointestinal Surgery, Department of General Surgery, Guangdong Provincial People's Hospital (Guangdong Academy of Medical Sciences), Southern Medical University, Guangzhou, China; [3]Center for Bariatric and Metabolic Surgery, Klinikum Ernst von Bergmann, Academic Hospital of the Charité-Universitätsmedizin Humboldt University Berlin, Potsdam, Germany; [4]Department of Gastrointestinal Surgery, Jieyang People's Hospital, Jieyang, China; [5]Shantou University Medical College, Shantou, China; [6]School of Medicine, South China University of Technology, Guangzhou, China

Contributions: (I) Conception and design: R Li, Z Yang, Y Li; (II) Administrative support: Z Yang, Y Li; (III) Provision of study materials or patients: All authors; (IV) Collection and assembly of data: All authors; (V) Data analysis and interpretation: R Li, Q Fan, X Lin, R Chen, B Luo; (VI) Manuscript writing: All authors; (VII) Final approval of manuscript: All authors.

[#]These authors contributed equally to this work as co-first authors.

Correspondence to: Zifeng Yang, MD. Department of Gastrointestinal Surgery, Department of General Surgery, Guangdong Provincial People's Hospital (Guangdong Academy of Medical Sciences), Southern Medical University, No. 106, Zhongshan 2nd Road, Guangzhou 510080, China. Email: yangzifeng@gdph.org.cn; Yong Li, MD, PhD. Department of Gastrointestinal Surgery, Department of General Surgery, Guangdong Provincial People's Hospital (Guangdong Academy of Medical Sciences), Southern Medical University, No. 106, Zhongshan 2nd Road, Guangzhou 510080, China; Guangdong Cardiovascular Institute, Guangdong Provincial People's Hospital, Guangdong Academy of Medical Sciences, Guangzhou, China. Email: liyong@gdph.org.cn.

Background: Management of peritoneal carcinomatosis (PC) remains a significant clinical challenge due to a lack of effective therapies. Pressurized intraperitoneal aerosol chemotherapy (PIPAC) has been identified as a safe and efficacious treatment for PC. However, despite the observed high potential for PIPAC in treating numerous PC cases, the technology is still limited in China. To address this deficit, we developed a novel nebulized drug delivery system (NDDS) and evaluated it in this study.

Methods: The NDDS was developed and was systematically assessed through tests of mechanical properties, granulometric analyses, sprayed distribution tests, and gravimetric analyses; moreover, drug penetration and distribution were examined *in vitro* and in a porcine model (female Tibetan pig).

Results: The NDDS, which included a high-pressure peristaltic pump, demonstrated a pressure initiation time of 5 s and a spray angle of 70°. Nebulization was consistent from the fifth second onward, with a median droplet diameter of 25.0–26.5 μm. The diameters of the sprayed intensive and expanded area were 26.1±1.4 and 48.5±1.0 cm at the vertical distance of 15 cm, and the stress generated was ≤3.790 Pa. Intraluminal drug distribution was extensive but heterogeneity, with 100- to 400-μm drug penetration depth (PD), and the optimal drug PD was observed in locations directly opposite to or adjacent surrounding the nozzle.

Conclusions: The developed NDDS demonstrated promising mechanical properties, effective granulometric characteristics, extensive spray coverage, and satisfactory drug penetration and distribution. It offers a practicable solution for the application of PIPAC and will hopefully improve the current dilemma in PC therapy.

Keywords: Pressurized intraperitoneal aerosol chemotherapy (PIPAC); nebulized drug delivery system (NDDS); granulometric characteristics; drug penetration; drug distribution

Submitted Dec 25, 2024. Accepted for publication Feb 03, 2025. Published online Feb 23, 2025.
doi: 10.21037/jgo-2024-1009
View this article at: https://dx.doi.org/10.21037/jgo-2024-1009

Introduction

Peritoneal carcinomatosis (PC) is widely recognized as the terminal stage of various solid tumors, whose prognosis is notably poor when treatment is limited to conventional systemic chemotherapy (1-5) due to the peritoneal-plasma barrier (6-9). The range of effective treatments for PC remains limited. Cytoreductive surgery (CRS) followed by hyperthermic intraperitoneal chemotherapy (HIPEC) has emerged as an effective treatment for PC (10-13), demonstrating the potential to improve patients' prognosis and quality of life (3,14-17). However, this advanced therapeutic intervention is associated with certain drawbacks, such as high concentrations of chemotherapeutic drugs, uneven distribution of drugs and heat within the abdomen, inadequate tissue penetration depth (PD), and an increased risk of postoperative complications (18-21), which taken together can restrict these indications for CRS + HIPEC therapy. In addition, CRS + HIPEC is inapplicable for patients with unresectable PC.

A recent innovation in treatment is pressurized intraperitoneal aerosol chemotherapy (PIPAC), which has been reported to be a safe and effective treatment for PC, especially for unresectable cases (22,23). This method strives to achieve a homogeneous spatial distribution of chemotherapy drugs, a superior depth of drug penetration, and higher local drug concentrations, which can reduce systemic toxicity and side effects (4,24-28). The conventional PIPAC procedure involves a machine equipped with a high-pressure syringe pump that was originally designed for clinical vascular angiography. However, this method also has some notable limitations, including the inconvenience and potential exposure risks associated with chemotherapeutic drug loading. PIPAC could be repeatedly performed and the routine interval time was 4–6 weeks, the stage of PC and the histological response to the treatment were assessed according to the peritoneal cancer index (PCI) (29) and the Peritoneal Regression Grading Score (PRGS) (30) in repeated PIPAC cycles, respectively.

According to recent epidemiological data (31), approximately 700,000 cases of PC were reported in China as of 2020, with 384,000 new cases being diagnosed each year, highlighting the pressing need for a greater focus on the large segment of the population with this disease. Despite a clear clinical need, the availability of PIPAC systems and specialized medical centers for PC treatment remains limited across China, and there is thus an urgent demand for a PIPAC system that can ensure stable performance while also ensuring safe and convenient drug loading.

Peristaltic pumps are widely applied in clinics due to their ability to minimize drug exposure risks, prevent contamination, and ensure output stability (32,33); thus,

Highlight box

Key findings

- The proposed novel nebulized drug delivery system (NDDS) demonstrated a maximum upstream pressure of 200–300 psi, a pressure initiation time of 5 s, a flow rate of 0.7 mL/s, a mean particle velocity of 22.7 m/s, and a spray angle of 70°.
- Nebulization was consistent from the fifth second onward, with a median droplet diameter of 25.0–26.5 μm and over 60% of particles being <30 μm.
- At different vertical distance (5–15 cm), the sprayed areas were extensive, deep staining, and homogeneous. The stress generated was ≤3.790 Pa, which was significantly lower than the damage stress threshold (>130 kPa).
- Intraluminal drug distribution was extensive, but heterogeneity was present at a drug penetration depth of 100–400 μm.

What is known and what is new?

- Pressurized intraperitoneal aerosol chemotherapy (PIPAC) based on the traditional syringe pump devices has been widely applied as a feasible, safe, and effective treatment for peritoneal carcinomatosis (PC), especially for unresectable PC; however, its use remains limited in China.
- The NDDS had satisfactory performance compared to other systems, with advantages of output stability and a lower risk of drug contamination or exposure; this approach can facilitate the popularization of PIPAC in China and improve PC treatment.

What is the implication, and what should change now?

- The NDDS offers a potential solution for the application of PIPAC and could represent a significant advancement in overcoming the current limitations in PC treatment. Furthermore, PIPAC should become an integral component of PC therapy, especially for unresectable PC.

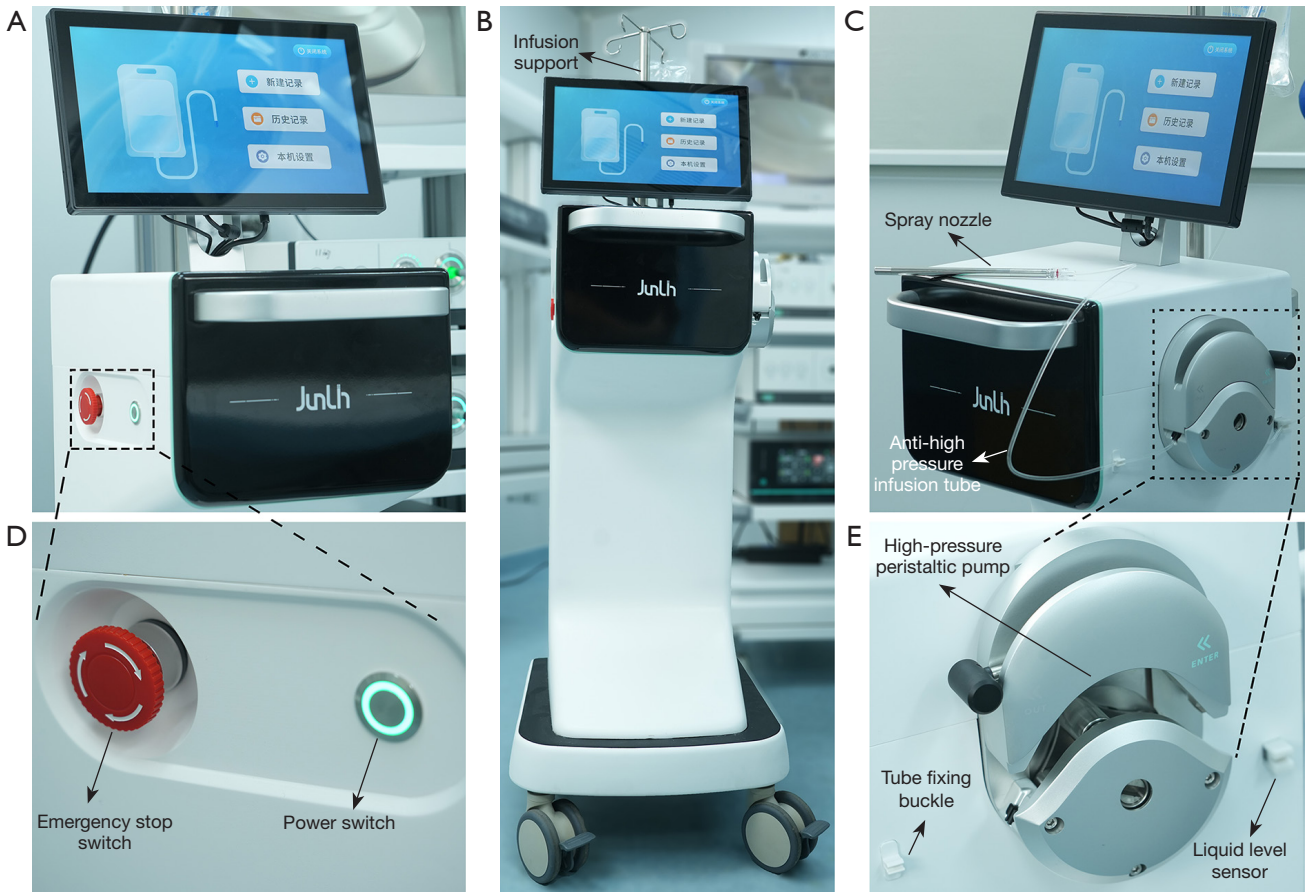

Figure 1 Illustration of the novel nebulized drug delivery system.

our research team collaborated with engineers to develop a novel nebulized drug delivery system (NDDS) that employs a high-pressure peristaltic pump. In order to demonstrate the applicability of NDDS for the PIPAC procedure, in this study, we evaluated the NDDS through laboratory tests, an *in vitro* model, and a porcine abdominal cavity model. We present this article in accordance with the ARRIVE reporting checklist (available at https://jgo.amegroups.com/article/view/10.21037/jgo-2024-1009/rc).

Methods

NDDS

The NDDS was developed, which includes a master computer (with an operating system) (*Figure 1A*), an infusion support (*Figure 1B*), an all-in-one unit that includes a spray nozzle (cat. no. JL-WP10-2.2; Junlin Medical Technology Co., Ltd., Guangzhou, China), an anti-high pressure infusion tube, and a puncture head (*Figure 1C*), an emergency stop switch (*Figure 1D*), a high-pressure peristaltic pump (China National Intellectual Property Administration Patent no. ZL 2023 1 0085133.2) and a liquid level sensor (*Figure 1E*). The liquid level sensor serves as a critical safety feature and is designed to halt nebulization once the infusion tube becomes empty, preventing excessive air insufflation into the abdominal cavity.

The operating system (cat no. V1, MCCX_PC_SW; Junlin Medical Technology Co., Ltd., Guangzhou, China) features high performance and ease of operation; for a detailed schematic, please see Figure S1A-S1H.

Mechanical properties

The maximum upstream pressure (MUP) and the pressure initiation time (PIT; the duration to reach MUP following the start of the machine) of the nebulized system are

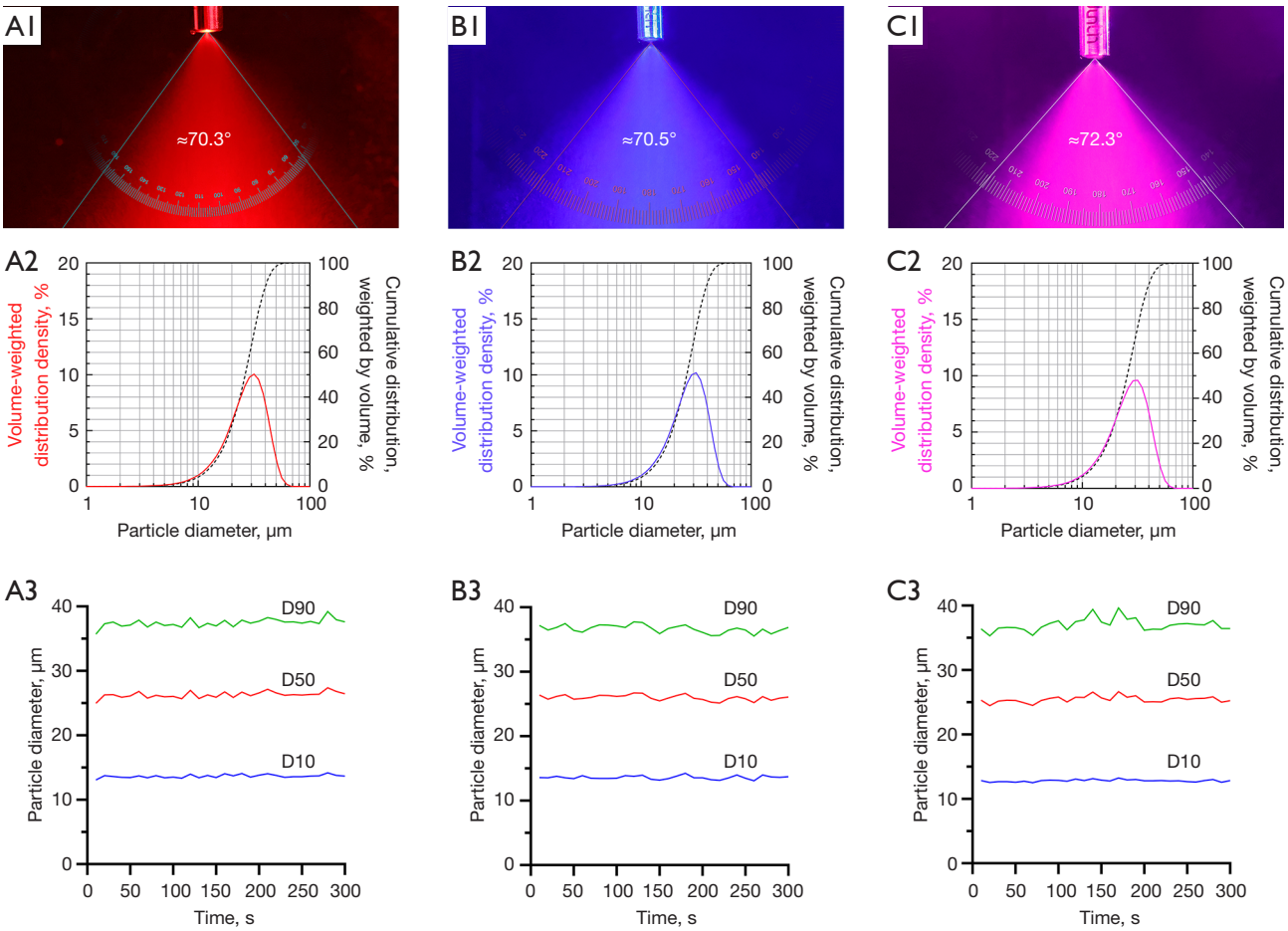

Figure 2 Granulometric analyses. Analyses were respectively performed for the sterile water (A_1-A_3), 0.9% NaCl (B_1-B_3), and 5%-glucose solution (C_1-C_3), including the sprayed cone angle (A_1-C_1), the aerosol particle size distribution (the Rosin-Rammler distribution) (A_2-C_2), and the change trend of the aerosol particle size during the 5-minute nebulization (A_3-C_3). D10, the 10th percentile.

quantified using a pressure transmitter. Concurrently, the flow velocity (V_D) of aerosol particles at the exit is determined using Eq. [1], representing the liquid flow rate (Q_L) to the smallest cross-sectional area (CSA) of the nozzle orifice (A_D) ratio (34). The d_D is the diameter of the nozzle orifice (200 μm).

$$v_D = \frac{Q_L}{A_D} = \frac{(4 \times Q_L)}{(\pi \times d_D^2)} < v_{D,\max} = \sqrt[2]{\frac{2 \times p_{MIP}}{\rho_L}} \quad [1]$$

The spray cone angle and nebulization pattern for sterile water, 0.9% NaCl solution, and 5%-glucose solution were documented photographically and assessed (*Figure 2*, A_1-C_1). The spray angle (2α) is calculated using the Eq. [2], where H is the vertical distance (cm) between the nozzle tip and the directly opposite sprayed coverage plane, while D is the diameter (cm) of the opposite coverage plane.

$$D = 2H \times \tan\left(\frac{\alpha}{2}\right) \quad [2]$$

Granulometric analyses

Granulometric analyses were performed with a laser particle size analyzer (Winner 311-XP, Jinan Winner Particle Instruments Stock Co., Ltd., Jinan, China) on sterile water, 0.9% NaCl, and 5%-glucose solution (Figure S2A). These solutions were nebulized continuously for 5 min, during which the granulometric distribution for each second was recorded (*Figure 2*, A_2-C_2). The maximal droplet sizes at the 10th percentile (D10), 50th percentile (D50), and 90th

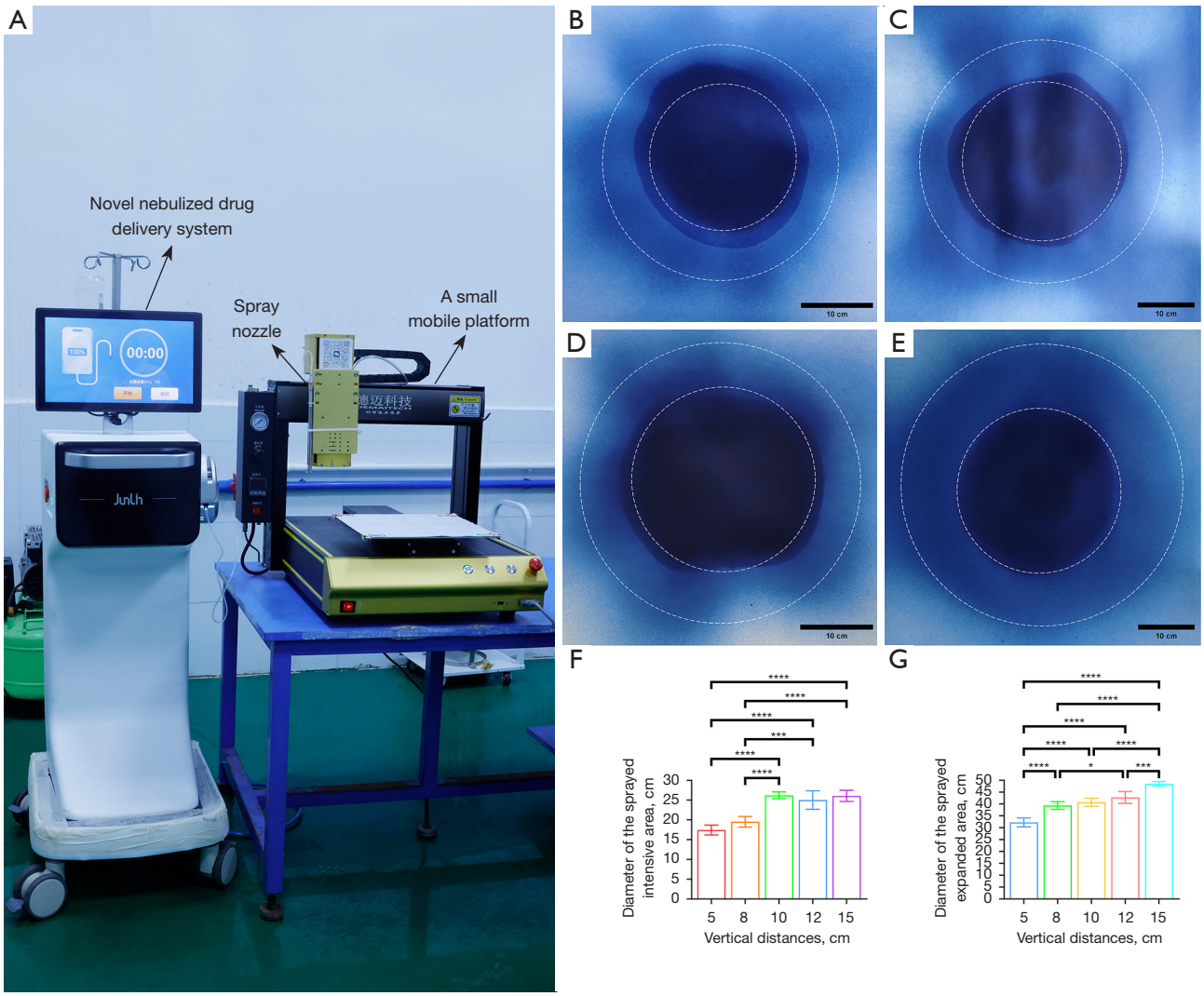

Figure 3 Sprayed distribution tests. An industrial test platform was established (A). The intensive and expanded sprayed area on vertical distances of 8 (B), 10 (C), 12 (D), and 15 (E) cm, and the respective differences among them (including a vertical distance of 5 cm) (F,G). *, P<0.05; ***, P<0.001; ****, P<0.0001.

percentile (D90) of the aerosolized particles were recorded. Trends in D10, D50, and D90 over the initial minute and the entire 5-minute period are presented in a line chart (weighted by volume) (*Figure 2*, A_3-C_3, Figure S2B-S2D). This analysis aimed to assess the aerosol's initial formation stage and the stability of aerosol generation. Each solvent was tested three times, with a new nozzle being employed for each test. Additionally, the particle size distribution was depicted using the Rosin-Rammler distribution (35), based on the mean particle size observed during the stable stage of the 5-minute nebulization period.

Sprayed distribution test

The distribution of spray was evaluated by quantifying the spread of methylene blue (MB) (1%; cat no. PGJ8024-W1; Pinggen Experimental Equipment Co., Ltd., Dongguan, China), which was sprayed on the blotting paper (BP). The nozzle was secured to a mobile platform (Demai Intelligent Technology Co., Ltd., Dongguan, China). The nozzle height was sequentially set to 5, 8, 10, 12, and 15 cm above the BP (*Figure 3A*). BPs (60 cm × 60 cm) were used as substrates, onto which a 30-mL MB solution was applied at a rate of 0.7 mL/s (4) except for the distances

of 5 cm, for which the BP was sprayed with 25 mL of MB (36). BPs were all dried at room temperature. Subsequently, the sprayed area (SA) on the BP was documented photographically, and the areas where MB was applied more densely (intensive area) and areas where it dispersed more broadly (expanded area) were distinguished (*Figure 3B-3E*, Figure S3). The diameter of SA was quantified using ImageJ software (https://imagej.net; ImageJ, US National Institutes of Health, Bethesda, MD, USA) (*Figure 3F,3G*). All measurements were conducted five times.

Gravimetric analyses

For gravimetric analyses, sterile water was sprayed through a nozzle inside a hermetic plastic bottle for 15 s, whose weight was measured as the actual value (W_a). Subsequently, the nozzle was attached to a mobile platform (Demai Intelligent Technology Co., Ltd., Dongguan, China), with the vertical distance set at 8 cm (*Figure 3A*) in accordance with the clinically established distance for the PIPAC procedure (37). Following this, sterile water was sprayed onto water writing cloth (WWC) for 15 s with the same nozzle, whose weight was measured as the depositional weight (W_d). The percentage of water deposited on the WWC was calculated as W_d/W_a. All measurements were conducted in triplicate.

The estimation of safety in clinical application

The safety of the aerosol sprayed on the directly opposing abdominal tissues or organs was determined based on the estimated stress (ES), which was calculated via Eq. [3].

$$ES = \frac{F}{A} = \frac{F}{\left(\pi \times \left(\frac{d}{2}\right)^2\right)} \quad [3]$$

In this equation, F is the impulsive force [Newton; (N)] of the spray on different linear distances (between the nozzle and the surface of measuring balance), including 5, 8, 10, and 12 cm, and was measured via a test instrument (cat. no. YN-FB150; Dongguan Nanyue Test Equipment Co., Ltd., Dongguan, China); additionally, A is the cross-sectional area (CSA) (m^2) of the sprayed aerosol cone that directly impacts the opposing surface, and the CSA was measured via the nebulization of sterile water on the WWC until the formation of a full suborbicular shape, which was performed on different vertical distances (5, 8, 10, and 12 cm) and all were photo-recorded with a scale bar every 1 s. Finally, π=3.14, and d is the diameter of the CSA. All measurements were performed in quintuplicate.

Ex vivo experiments

Hermetic box model

A commercially airtight cuboid-shaped plastic box (volume =3.5 L) was applied to mimic the abdominal cavity of human patients (3–5 L). Borg 10- and a 5-mm balloon trocars (Hangzhou Kangji Medical Instrument Co., Ltd., Hangzhou, China) were inserted and secured at the cover plate via the sealing rings, which was respectively prepared for the 10-mm nozzle and the electronic thermometer (cat. no. KT300L; OUDASHI Technology Co., Ltd., Chaozhou, China) that was applied for the in-box temperature monitoring. Inside the model, four fresh excised porcine peritoneal tissues (3 cm × 3 cm × 0.5 cm) with the peritoneal side up were placed on the location directly opposite to the nozzle orifice (position A), the medial wall (position C), the top ceiling (position D), and the location beside the position A which was covered with an arc-shaped plastic plate (position B), respectively (Figure S4A).

After the model with 12-mmHg of internal pressure was established, it was submerged in distilled water maintained at 36.0–37.0 ℃. This temperature was kept constant and monitored in real time with an electromagnetic heater (JB-2, Changzhou Aohua Instrument Co., Ltd., Changzhou, China) and an electronic thermometer (cat. no. KT300L; OUDASHI Technology Co., Ltd., Chaozhou, China). Subsequently, 50 mL of 0.9% NaCl containing 3.0 mg of doxorubicin was aerosolized and maintained at 12 mmHg of pressure for 30 minutes inside the model, and the vertical distance of nozzle was 8 cm. Finally, the chemotherapeutic aerosol was evacuated using a hermetic vacuum extractor. The doxorubicin nebulized experiment was performed in triplicate.

Collection and management of specimen

After the surface was washed with 0.9% NaCl, four specimens were carefully collected and immediately stored in the liquid nitrogen. Four 0.5 cm × 0.5 cm × 0.5 cm samples were then randomly obtained from each deep-frozen biopsy specimen, which were respectively prepared for the paraffin section (n=1) and cryosections (n=3), with each sample only being prepared for a single section

(thickness =8 μm). The paraffin section was stained with hematoxylin and eosin to reveal the peritoneal side of the tissue, while the cryosections which were stained with 2.0 μg/mL of 4',6-diamidino-2-phenylindole (DAPI) to measure the doxorubicin PD.

Drug penetration

The PD was defined as the distance from the peritoneal surface to the level at which the bulk of the accumulated fluorescence was last visible. All cryosections were scanned using the Pannoramic MIDI Digital Slide Scanner (3DHISTECH, Budapest, Hungary), and the autofluorescence of doxorubicin at an excitation wavelength of 490 nm and an emission wavelength of 560 to 590 nm was observed. The drug PD for each cryosection was measured using CaseViewer version 2.4.0 software (3DHISTECH) under a magnification of ×20 (Figure S4B). Measurements at three random points on each cryosection were performed by an experienced pathologist.

In vivo experiments

Establishment of the experimental platform

In the laminar flow operating room, after general anesthesia and tracheal intubation, healthy and normally feeding Tibetan pigs (females, weighing 40 kg) were placed in the supine position, which was provided by the Guangdong Bright Pearl Biotechnology Co., Ltd. [license number: SCXK(Yue)2022-0061]. Two 10-mm balloon trocars were symmetrically placed on the two sides of the umbilicus after skin preparation and draping were completed. The NDDS was placed on the left side of the porcine, and the 10-mm nozzle and the laparoscope (OptoMedic Technology Co., Ltd., Foshan, China) were respectively introduced into the homolateral and the contralateral trocars (*Figure 4A*).

Drug distribution and PD

A postmortem specimen and a living porcine model were each subjected to 1% intraperitoneal pressurized MB (150 mL) and nebulization of doxorubicin (50 mL of 0.9% NaCl containing 3.5 mg doxorubicin) solution (*Figure 4B*) at a flow rate of 0.7 mL/s, working pressure of 200–300 psi, and a pneumoperitoneum pressure of 12 mmHg, which was maintained for 30 minutes after nebulization. Finally, all of the drug aerosol was evacuated via a hermetic vacuum extractor.

In the nebulized MB experiment, the drug distribution was evaluated via the observation of the blue staining inside the abdominal cavity (38,39). Meanwhile, in the doxorubicin nebulized experiment, after the euthanasia of pig, three peritoneal specimens (3 cm × 3 cm × 2 cm) were randomly biopsied in each region of the abdominal cavity according to the modified PCI score (39), along with the gastric wall, uterus, and mesovarium. After the surface was washed by 0.9% NaCl and packed into the centrifuge tubes with labels, all specimens were stored in liquid nitrogen. Random sampling of the specimens was performed (four 0.5 cm × 0.5 cm × 2 cm samples were randomly obtained from each specimen), and the preparation, management, scanning of pathological sections, and the observation and measurement of the doxorubicin fluorescence were all performed in a similar fashion to that of the *in vitro* experiments, with the spatial distribution of the drug inside the porcine abdominal cavity being assessed (*Figure 4*, C_1-C_{14}). As the existing validated PIPAC devices are unavailable in China, comparison with a control group was not possible. Therefore, inclusion and exclusion criteria for experimental animals were not applicable.

Occupational safety

Doxorubicin was a cytotoxic drug and harmful to healthy medical staffs. Therefore, in the *ex vivo* and *in vivo* experiments, standard operation, moderate intraperitoneal pressure, appropriate abdominal wall incisions, application of balloon trocars and which were completely covered by the wet gauze were all key points to preventing rapid leakage of chemotherapeutic drugs.

Ethical statement

All animal experiments of this study were performed in the animal experimental centre of Guangzhou Huateng Biomedical Technology Co., Ltd. Animal experiments were performed under a project license (No. b202308-14) approved by the Animal Ethics Committee of Guangzhou Huateng Biomedical Technology Co., Ltd., in compliance with institutional guidelines for the care and use of animals. A protocol was prepared before the study but was not registered.

Statistical analyses

All experimental data were recorded and collated using Excel (Microsoft Corp., Redmond, WA, USA). Continuous variables are expressed as the mean ± standard deviation

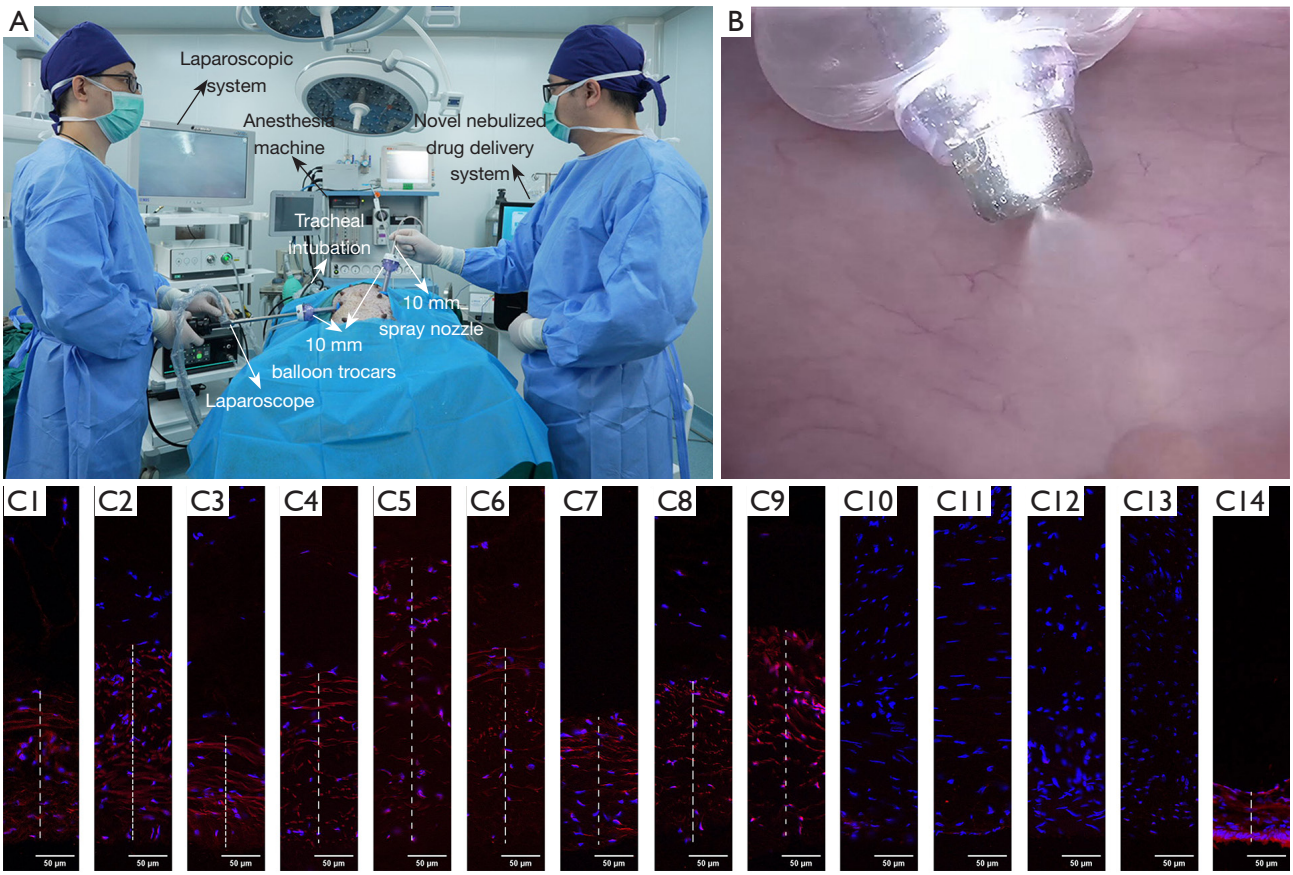

Figure 4 *In vivo* experiments. A porcine experimental platform was established (A), in which 3.5 mg of doxorubicin in 50 mL of 0.9% saline was nebulized (B). The doxorubicin fluorescence penetration of parietal peritoneum on the abdominal central (C_1), right upper (C_2), epigastrium (C_3), left upper (C_4), left flank (C_5), left lower (C_6), pelvic (C_7), right lower (C_8), and right flank regions (C_9) and of the visceral peritoneum of the stomach (C_{10}), small intestine (C_{11}), colon (C_{12}), uterus (C_{13}), and mesovarium (C_{14}).

(SD) or as the median and range. Data analyses were performed via SPSS 26 (IBM Corp., Armonk, NY, USA). The comparison of means between different groups (≥3 groups) was performed with one-way ANOVA analysis, and the plotting of results from the granulometric analyses, sprayed distribution tests, and *in vitro* experiments were conducted via GraphPad Prism 9.5.1 (GraphPad Software Inc., Boston, MA, USA). P<0.05 was considered to indicate a statistically significant difference.

Results

Mechanical properties

The MUP range was 200–300 psi, with a PIT of approximately 5 seconds. The flow rate was 0.7 mL/s, and the particle velocity from the nozzle was approximately 22.7 m/s. The spray angle of different solutions through the nozzle was around 70° (*Figure 2*, A_1-C_1).

Granulometric analyses

Regardless of the type of solvents, after the initial 4 seconds, the aerosol generative process was finally stable at the fifth second (Figure S2B-S2D). For sterile water, 0.9% NaCl, and 5%-glucose solution, in the stable phase, the median droplet diameter (D50) was 25.3±1.0, 26.4±0.3, and 26.3±1.2 μm, respectively (*Figure 2*, A_2-C_2, Table S1). The D10, D50, and D90 measurements showed minimal fluctuation throughout the stable 5-minute nebulization period (*Figure 2*, A_3-C_3); moreover, the percentage of aerosolized particles smaller than 30 μm was 68.8%±5.1%, 63.7%±1.2%, and 63.3%±4.5%, respectively (Table S1).

Table 1 The sprayed distribution area of spray nozzles from different countries

Spray nozzles	Country	Vertical distance (cm)	Sprayed solution	Sprayed volume (mL)	Sprayed distribution area*		Reference
					Intensive area (cm)	Expanded area (cm)	
JunLin	China	5	MB	25	17.4±1.3	32.3±1.9	–
		8	MB	30	19.5±1.3	39.4±1.6	
		10	MB	30	26.2±0.9	40.7±1.7	
		12	MB	30	25.0±2.3	42.8±2.5	
		15	MB	30	26.1±1.4	48.5±1.0	
Capnopen® (initial nebulizer)	Germany	15	BI	30	10.0	NA	(34)
Capnopen® (advanced nebulizer)	Germany	5	MB	25	12.2	15.7	(36)
		10	MB	25	12.5	19.0	
		15	MB	25	12.3	22.0	
Dreampen®	Korea	12	MB	30	18.5	28.3	(40)

*, the sprayed distribution size from the present study is expressed as mean ± standard deviation, while the data from previous studies are expressed as mean due to their nonuniform formatting. MB, methylene blue; BI, blue ink; NA, not available.

Sprayed distribution and gravimetric analyses

At the vertical distance of 15 cm, the average diameter of the sprayed intensive area (SIA) and sprayed expanded area (SEA) was 26.1±1.4 and 48.5±1.0 cm, respectively (*Figure 3E*, *Table 1*); the other results are displayed in *Table 1*, *Figure 3*, and Figure S3. Statistically significant differences were observed between 5 or 8 cm and any other distances of the SIA except for the difference between 5 and 8 cm (*Figure 3F*) and between all different distances of the SEA except for differences between 8 and 10 cm and between 10 and 12 cm (*Figure 3G*).

In the gravimetric analyses, at the distance of 8 cm (37), the average deposition rate of sterile water was 88.2%±3.6% (Table S2).

Estimated safety of clinical nebulization

A full suborbicular shape on the WWC was preliminarily formed in the 5–7 s after nebulization regardless of the distance, which was considered to be the CSA of the sprayed aerosol. The ES of the spray from the nozzle orifice was 3.790, 1.269, 0.846, and 0.791 Pa at distances of 5, 8, 10, and 12 cm, respectively (Table S3).

In vitro experiments

At positions A, B, C, and D, the average drug PDs were 291.4±30.2, 186.0±37.7, 273.5±35.2, and 189.2±51.5 μm (Table S4), respectively, which were statistically different from each other except for the difference between position B and D (Figure S4B).

In vivo experiments

Extensive, deep, and homogeneous blue staining could be significantly observed on the surface of different tissues and organs inside the porcine abdominal cavity (Figure S5A-S5F). Meanwhile, there were no intraoperative adverse events (bleeding, perforation, death, etc.), and the drug PDs ranged from 100- to 400-μm were observed in different regions of the porcine peritoneal cavity except for the visceral peritoneum which covered on the stomach, small intestine, colon, and uterus (*Figure 4*, C_{10}-C_{13}); moreover, the left and right flank regions exhibited the most optimal drug PDs, followed by the right upper, left upper, right lower, left lower, central, pelvis, epigastrium, and mesovarium (*Figure 4*, C_1-C_9 and C_{14}, *Table 2*).

Discussion

The mechanical properties of the proposed NDDS, including the MUP (200–300 psi) and the spray cone angle (70°) were consistent with those of the previously reported PIPAC devices (4,34,41,42). However, differences

Table 2 The depth of the doxorubicin penetration in the experimental porcine model

Sampling position	Depth of the drug penetration (μm)	
	Median (range)	Mean ± SD
Central	197.6 (181.3–226.8)	202.4±15.6
Right upper	232.9 (199.2–256.4)	228.0±17.2
Epigastrium	118.1 (101.1–140.8)	119.0±11.4
Left upper	224.8 (196.2–263.6)	228.1±16.4
Left flank	321.0 (245.0–379.5)	316.5±33.2
Left lower	201.6 (182.4–308.9)	207.9±23.6
Pelvis	153.3 (103.9–206.8)	152.5±37.5
Right lower	207.8 (153.7–256.5)	204.6±20.1
Right flank	277.9 (251.5–321.6)	280.8±22.6
Stomach	0	0
Small intestine	0	0
Colon	0	0
Uterus	0	0
Mesovarium (full layer)	66.9 (45.3–115.9)	70.5±17.5

SD, standard deviation.

were observed in the PIT (5 s), flow rate (0.7 mL/s), and the particle velocity (22.7 m/s). The PIT of the NDDS was significantly shorter than that reported in previous studies (18–100 s) (41,42), indicating that the high-pressure peristaltic pump could achieve the necessary working pressure in an exceptionally brief period (5 s). This efficiency is attributable to the pressure-priority control system that emphasizes the stability of the aerosol particle size and composition. Consequently, the NDDS may offer advantages for PIPAC therapy over the flow-priority control system of the high-pressure syringe pump (41,42), which was originally developed for clinical angiography applications.

The flow rate and the particle velocity were higher than those reported for previous PIPAC devices (34,40-42), and they could be considered as potential risk factors for abdominal tissue or organ damage during PIPAC nebulization. Consequently, a crucial but rarely discussed mechanical parameter—the stress of the sprayed liquid on the directly opposing surface—was thoroughly evaluated and discussed in this context (43-46). According to our results, the ES of sprayed aerosol generated by the NDDS, ranging from 0.791 to 3.790 Pa, was within the safe tolerance range for abdominal tissues and organs. This is because these stresses were significantly lower than the damage stress threshold (>130 kPa) reported in related studies (43-46).

Granulometric analyses were conducted using three solutions commonly used in clinical settings as pharmaceutical solvents with representativeness and practical value. For all the solvent types, the initial phase of aerosol generation in the NDDS lasted only 4 s, a duration consistent with that of previously described devices (34). This brief initial phase quickly transitions to a stable aerosol generation stage, which typically continues for approximately 5 min (4). During this stable phase, the particle size distribution, indicated by the D10, D50, and D90 values, remained consistent, which is crucial for the efficacy of PIPAC therapy (47). The median particle size was found to be between 25.3 and 26.4 μm, aligning with findings from previous studies (34,41,42), and over 60% of the aerosol particles were smaller than 30 μm. These granulometric analysis results suggest that aside from electrophoresis and thermophoresis, the primary deposition mechanisms for the majority of aerosol particles generated by the proposed NDDS likely involve inertial impaction and gravitational settling (34). Further, outcomes from a computational fluid dynamics (CFD) model to simulate the PIPAC process suggested that under conditions of a 0.7-mL/s flow rate and more than 90% of particles being ≤40 μm in size (47), the aerosol particles generated by the NDDS could potentially cover the vast majority of the abdominal cavity, specifically the lower three-quarters.

The formation of the SIA and the SEA results from the direct deposition of mass aerosol particles from the nozzle through the inertial impaction and gravitational settling (34) and the deposition of floating aerosol particles due to turbulence and deflectional droplets following collision (48,49), respectively. In laboratory research, both the extent of the SEA and the uniformity of MB staining within the SIA can preliminarily predict and estimate the nebulized efficacy and drug distribution of the nebulized system in animal or human experiments. A more broadly sprayed area and deeper and more uniform staining suggest improved outcomes (40). For our proposed NDDS, sprayed areas at various vertical distances were uniformly quasicircular, with consistent and deep MB staining, markedly exceeding the dimensions reported in previous studies (34,36,40-42) under comparable experimental conditions. Meanwhile, the increased vertical distances meant a continuously expansive SEA but a non-incremental

SIA when a 10-cm distance was exceeded. At the clinically established distance (8 cm), the NDDS demonstrated a comparable deposition rate for sterile water (88.2%±3.6%) to the previous study (34), indicating that over 88% of the sprayed volume could directly impact and be deposited on the peritoneum or abdominal organs facing the nozzle orifice during the PIPAC procedure. These results suggest that the proposed NDDS could potentially offer nebulized efficacy and drug distribution within the abdominal cavity of animals or humans that is at least as effective as those of existing systems.

Tissue drug penetration is one of the essential prerequisites for ensuring the efficacy of intraperitoneal chemotherapy and significantly influences therapeutic outcomes (50). Previous studies have shown favorable tissue drug PDs (~2,000 μm) with the PIPAC procedure in both animal models and patients (37,51,52). The key determinants of PD include abdominal pressure (mmHg), temperature (℃), aerosol particle size (μm), vertical distance of the nozzle (cm), and stress (Pa) (50). In line with the three principles for animal experiments established by Russell and Burch (53,54)—replacement, reduction, and refinement—drug PD was initially investigated using a mature *in vitro* model consisting of a hermetic plastic box with a volume of 3.5 L (37,55,56). The experimental results demonstrated that first, the drug distribution of the proposed NDDS was heterogeneous, but the aerosol of chemotherapeutic drugs could effectively influence the porcine peritoneum with a 100- to 300-μm PD. Second, as compared to that of previous studies, the drug PD of the location directly opposite to the nozzle was comparable, while results from other positions were superior (37,55,56); this could be attributable to the shorter PIT, higher flow rate, greater extent of sprayed area of the NDDS, heating, and/or the peritoneum being from different types of porcine model (34,37,42,55,56).

The heterogeneity of aerosol drug distribution was demonstrated in the animal experiments; However, the extensive spatial distribution of the drug and the sufficient tissue drug penetration (100–400 μm) of the NDDS was confirmed via the MB and doxorubicin nebulized experiments, respectively, all of which were found to be non-inferior to those of existing clinical PIPAC systems (38,39,57); moreover, the chemotherapeutic drug spatial distribution inside patients' abdominal cavity could be estimated. Interestingly, only a few segmental drug penetrations were observed in the visceral peritoneum and were classified as nonpenetrations of doxorubicin; in contrast, there was continuous, full-layer drug penetration uniformly throughout the parietal peritoneum, and this may be attributable to the difference in histologic type between the parietal and visceral peritoneum (39) and/or the random sampling of the extensive visceral peritoneum.

Moreover, although the intraluminal drug distribution was characteristic of heterogenetic, some improvements of the present NDDS should not be ignored, such as much shorter pressure initial time, fast time to reach stable aerosol generative stage, and more extensive sprayed distribution area, which potentially improve the aerosol drug delivery. Beyond that, several issues still need to be addressed, like reducing the aerosol particle size but maintaining the satisfactory flow rate, particle velocity, and spray angle (47); developing the multi-nozzle nebulizer (42) or rotational sprayed nozzle (39); combining with the static electricity (58) or high temperature (41–43 ℃) (59). Especially, hyperthermic PIPAC (HPIPAC) might potentially improve the efficacy, its feasibility and safety had been demonstrated in the *in vivo* experiments, but the development was still limited due to its size and lack of drug research (59). However, this study mainly aimed to introduce a novel NDDS, and evaluated its potentially feasible and safe application for the standard PIPAC procedure, finally filling in the domestic blanks of PIPAC. Therefore, HPIPAC will be mainly explored and developed in subsequent investigations.

Furthermore, intraperitoneal chemotherapies have been performed for decades, limitations on the efficacy include: the intraperitoneal chemotherapy was restricted to lesions in the abdominal cavity due to the peritoneal-plasma barrier (60); therapeutic drugs inside the peritoneal cavity will be metabolized and cleared in several days (39); the traditional PIPAC treatment in clinic was rarely related to the immunotherapy. Therefore, further coping strategies included: first, PIPAC has to be synchronously combined with the systemic chemotherapy; second, innovative injectable hydrogels, nanoparticles, or probes should be developed as the agents for the chemotherapeutic drugs, in order to improve the drug spatial distributions and achieve the drug sustained release; third, oncolytic virus, CAR-T, anti-PD-1 and anti-PD-L1 drugs could combine with the PIPAC procedure.

The study involved several limitations which should be acknowledged. First, due to the fixed maximal upstream pressure and flow rate of the new system, assessing the relationship between the aerosol generation process and varying working pressures or volumetric flow rates was

not feasible. Second, the intraperitoneal pressure, the vertical distance of the nozzle, and the temperature during *ex vivo* and *in vivo* experiments were all changeless in this study, which all potentially affect the drug distribution and penetration of traditional PIPAC, and should be further evaluated in detail. Third, as the work was comprised of preliminary laboratory and animal investigations, the findings require further validation in clinical trials, especially in terms of therapeutic efficacy. Finally, a comparison between our proposed NDDS and other validated PIPAC devices could not be conducted due to the unavailability of these systems in China at the time of the study.

Conclusions

The NDDS demonstrated favorable mechanical properties, including rapid pressure initiation, a safe degree of stress, satisfactory granulometric characteristics—such as suitable aerosol particle size and stable aerosol generation—extensive spray coverage, and adequate drug penetration and distribution. These features indicate its applicability for clinical PIPAC therapy, offering hope for enhancing the currently used approaches in PC treatment.

Acknowledgments

Language editing for the manuscript was provided by Dr. Sharvesh Raj Seeruttun (State Key Laboratory of Oncology in South China, Collaborative Innovation Center for Cancer Medicine, Guangzhou, China); statistical guidance and support were provided by Dr. Wenjun He (Center for World Health Organization Studies and Department of Health Management, School of Health Management of Southern Medical University, Guangzhou, China); research and development and technical support were provided by the Guangzhou Junlin Medical Technology Co., Ltd.; the guidance in theoretical fluid mechanics was provided by Dr. Huanliang Zhang (MOE Key Laboratory of Disaster Forecast and Control in Engineering, Institute of Applied Mechanics, Jinan University, Guangzhou, China); and guidance in the theoretical knowledge of physics was provided by Prof. Jie Zhang (School of Mechanics and Construction Engineering, Jinan University, Guangzhou, China).

Footnote

Reporting Checklist: The authors have completed the ARRIVE reporting checklist. Available at https://jgo.amegroups.com/article/view/10.21037/jgo-2024-1009/rc

Data Sharing Statement: Available at https://jgo.amegroups.com/article/view/10.21037/jgo-2024-1009/dss

Peer Review File: Available at https://jgo.amegroups.com/article/view/10.21037/jgo-2024-1009/prf

Funding: This work was supported by the National Natural Science Foundation of China (No. 32370836), the NSFC Incubation Project of Guangdong Provincial People's Hospital (No. KY0120220049), and the Natural Science Foundation of Guangdong Province (No. 2023A1515110294).

Conflicts of Interest: All authors have completed the ICMJE uniform disclosure form (available at https://jgo.amegroups.com/article/view/10.21037/jgo-2024-1009/coif). All authors report that this work was supported by the National Natural Science Foundation of China (No. 32370836), the NSFC Incubation Project of Guangdong Provincial People's Hospital (No. KY0120220049), and the Natural Science Foundation of Guangdong Province (No. 2023A1515110294). The authors have no other conflicts of interest to declare.

Ethical Statement: The authors are accountable for all aspects of the work in ensuring that questions related to the accuracy or integrity of any part of the work are appropriately investigated and resolved. Animal experiments were performed under a project license (No. b202308-14) approved by the Animal Ethics Committee of Guangzhou Huateng Biomedical Technology Co., Ltd., in compliance with institutional guidelines for the care and use of animals.

References

1. Lambert LA. Looking up: Recent advances in

understanding and treating peritoneal carcinomatosis. CA Cancer J Clin 2015;65:284-98.
2. Franko J, Shi Q, Meyers JP, et al. Prognosis of patients with peritoneal metastatic colorectal cancer given systemic therapy: an analysis of individual patient data from prospective randomised trials from the Analysis and Research in Cancers of the Digestive System (ARCAD) database. Lancet Oncol 2016;17:1709-19.
3. Foster JM, Zhang C, Rehman S, et al. The contemporary management of peritoneal metastasis: A journey from the cold past of treatment futility to a warm present and a bright future. CA Cancer J Clin 2023;73:49-71.
4. Alyami M, Hübner M, Grass F, et al. Pressurised intraperitoneal aerosol chemotherapy: rationale, evidence, and potential indications. Lancet Oncol 2019;20:e368-77.
5. Coccolini F, Gheza F, Lotti M, et al. Peritoneal carcinomatosis. World J Gastroenterol 2013;19:6979-94.
6. Guchelaar NAD, Noordman BJ, Koolen SLW, et al. Intraperitoneal Chemotherapy for Unresectable Peritoneal Surface Malignancies. Drugs 2023;83:159-80.
7. Flessner MF. The transport barrier in intraperitoneal therapy. Am J Physiol Renal Physiol 2005;288:F433-42.
8. Ren K, Xie X, Min T, et al. Development of the Peritoneal Metastasis: A Review of Back-Grounds, Mechanisms, Treatments and Prospects. J Clin Med 2022;12:103.
9. Jacquet P, Sugarbaker PH. Peritoneal-plasma barrier. In: Sugarbaker PH, editor. Peritoneal Carcinomatosis: Principles of Management. Boston, MA: Springer US; 1996. p. 53-63.
10. Yoshino T, Cervantes A, Bando H, et al. Pan-Asian adapted ESMO Clinical Practice Guidelines for the diagnosis, treatment and follow-up of patients with metastatic colorectal cancer. ESMO Open 2023;8:101558.
11. Shitara K, Fleitas T, Kawakami H, et al. Pan-Asian adapted ESMO Clinical Practice Guidelines for the diagnosis, treatment and follow-up of patients with gastric cancer. ESMO Open 2024;9:102226.
12. Adamina M, Warlaumont M, Berger MD, et al. Comprehensive Treatment Algorithms of the Swiss Peritoneal Cancer Group for Peritoneal Cancer of Gastrointestinal Origin. Cancers (Basel) 2022;14:4275.
13. Vaira M, Robella M, Guaglio M, et al. Diagnostic and Therapeutic Algorithm for Appendiceal Tumors and Pseudomyxoma Peritonei: A Consensus of the Peritoneal Malignancies Oncoteam of the Italian Society of Surgical Oncology (SICO). Cancers (Basel) 2023;15:728.
14. Filis P, Mauri D, Markozannes G, et al. Hyperthermic intraperitoneal chemotherapy (HIPEC) for the management of primary advanced and recurrent ovarian cancer: a systematic review and meta-analysis of randomized trials. ESMO Open 2022;7:100586.
15. Zhang JF, Lv L, Zhao S, et al. Hyperthermic Intraperitoneal Chemotherapy (HIPEC) Combined with Surgery: A 12-Year Meta-Analysis of this Promising Treatment Strategy for Advanced Gastric Cancer at Different Stages. Ann Surg Oncol 2022;29:3170-86.
16. Ali YM, Sweeney J, Shen P, et al. Effect of Cytoreductive Surgery and Hyperthermic Intraperitoneal Chemotherapy on Quality of Life in Patients with Peritoneal Mesothelioma. Ann Surg Oncol 2020;27:117-23.
17. Shan LL, Saxena A, Shan BL, et al. Quality of life after cytoreductive surgery and hyperthermic intra-peritoneal chemotherapy for peritoneal carcinomatosis: A systematic review and meta-analysis. Surg Oncol 2014;23:199-210.
18. Aherne EA, Fenlon HM, Shields CJ, et al. What the Radiologist Should Know About Treatment of Peritoneal Malignancy. AJR Am J Roentgenol 2017;208:531-43.
19. Pelz JO, Doerfer J, Hohenberger W, et al. A new survival model for hyperthermic intraperitoneal chemotherapy (HIPEC) in tumor-bearing rats in the treatment of peritoneal carcinomatosis. BMC Cancer 2005;5:56.
20. Beeharry MK, Liu WT, Yao XX, et al. A critical analysis of the cytoreductive surgery with hyperthermic intraperitoneal chemotherapy combo in the clinical management of advanced gastric cancer: an effective multimodality approach with scope for improvement. Transl Gastroenterol Hepatol 2016;1:77.
21. Dohan A, Hobeika C, Najah H, et al. Preoperative assessment of peritoneal carcinomatosis of colorectal origin. J Visc Surg 2018;155:293-303.
22. Orgad R, Bakrin N, Bonnefoy I, et al. Number of Pressurized Intraperitoneal Aerosol Chemotherapy (PIPAC) Treatments is Associated with Longer Survival: Analysis of a Large Prospective Cohort of Patients With Unresectable Peritoneal Surface Malignancies. Ann Surg 2024. [Epub ahead of print]. doi: 10.1097/SLA.0000000000006447.
23. Rauwerdink P, van de Vlasakker VCJ, Wassenaar ECE, et al. First-line palliative systemic therapy alternated with oxaliplatin-based pressurized intraperitoneal aerosol chemotherapy for unresectable colorectal peritoneal metastases: A single-arm phase II trial (CRC-PIPAC-II). Eur J Surg Oncol 2024;50:108487.
24. Grass F, Vuagniaux A, Teixeira-Farinha H, et al. Systematic review of pressurized intraperitoneal aerosol chemotherapy for the treatment of advanced peritoneal carcinomatosis.

Br J Surg 2017;104:669-78.
25. Di Giorgio A, Macrì A, Ferracci F, et al. 10 Years of Pressurized Intraperitoneal Aerosol Chemotherapy (PIPAC): A Systematic Review and Meta-Analysis. Cancers (Basel) 2023;15:1125.
26. Taliento C, Restaino S, Scutiero G, et al. Pressurized intraperitoneal aerosol chemotherapy (PIPAC) with cisplatin and doxorubicin in patients with ovarian cancer: A systematic review. Eur J Surg Oncol 2023;49:107250.
27. Case A, Prosser S, Peters CJ, et al. Pressurised intraperitoneal aerosolised chemotherapy (PIPAC) for gastric cancer with peritoneal metastases: A systematic review by the PIPAC UK collaborative. Crit Rev Oncol Hematol 2022;180:103846.
28. Lordick F, Carneiro F, Cascinu S, et al. Gastric cancer: ESMO Clinical Practice Guideline for diagnosis, treatment and follow-up. Ann Oncol 2022;33:1005-20.
29. Jacquet P, Sugarbaker PH. Clinical research methodologies in diagnosis and staging of patients with peritoneal carcinomatosis. Cancer Treat Res 1996;82:359-74.
30. Solass W, Sempoux C, Detlefsen S, et al. Peritoneal sampling and histological assessment of therapeutic response in peritoneal metastasis: proposal of the Peritoneal Regression Grading Score (PRGS). Pleura Peritoneum 2016;1:99-107.
31. Yang R, Su YD, Ma R, et al. Clinical epidemiology of peritoneal metastases in China: The construction of professional peritoneal metastases treatment centers based on the prevalence rate. Eur J Surg Oncol 2023;49:173-8.
32. Forouzandeh F, Alfadhel A, Arevalo A, et al. A review of peristaltic micropumps. Sens Actuators A Phys 2021;326:112602.
33. Formato G, Romano R, Formato A, et al. Fluid–Structure Interaction Modeling Applied to Peristaltic Pump Flow Simulations. Machines 2019;7:50.
34. Göhler D, Khosrawipour V, Khosrawipour T, et al. Technical description of the microinjection pump (MIP(®)) and granulometric characterization of the aerosol applied for pressurized intraperitoneal aerosol chemotherapy (PIPAC). Surg Endosc 2017;31:1778-84.
35. Dunbar CA, Hickey AJ. Evaluation of probability density functions to approximate particle size distributions of representative pharmaceutical aerosols. J Aerosol Sci 2000;31:813-31.
36. Toussaint L, Sautkin Y, Illing B, et al. Comparison between microcatheter and nebulizer for generating Pressurized IntraPeritoneal Aerosol Chemotherapy (PIPAC). Surg Endosc 2021;35:1636-43.
37. Khosrawipour V, Khosrawipour T, Falkenstein TA, et al. Evaluating the Effect of Micropump© Position, Internal Pressure and Doxorubicin Dosage on Efficacy of Pressurized Intra-peritoneal Aerosol Chemotherapy (PIPAC) in an Ex Vivo Model. Anticancer Res 2016;36:4595-600.
38. Mun J, Park SJ, Kim HS. Rotational intraperitoneal pressurized aerosol chemotherapy in a porcine model. Gland Surg 2021;10:1271-5.
39. Park SJ, Lee EJ, Lee HS, et al. Development of rotational intraperitoneal pressurized aerosol chemotherapy to enhance drug delivery into the peritoneum. Drug Deliv 2021;28:1179-87.
40. Lee HS, Kim J, Lee EJ, et al. Evaluation of a Novel Prototype for Pressurized Intraperitoneal Aerosol Chemotherapy. Cancers (Basel) 2020;12:633.
41. Daniel G, Kathrin O, Mehdi O, et al. Comparative Analysis of Nebulizers in Clinical use for Pressurized Intraperitoneal Aerosol Chemotherapy (PIPAC). medRxiv 2023:2023.03.24.23287646.
42. Göhler D, Oelschlägel K, Ouaissi M, et al. Performance of different nebulizers in clinical use for Pressurized Intraperitoneal Aerosol Chemotherapy (PIPAC). PLoS One 2024;19:e0300241.
43. Khan AF, Macdonald MK, Streutker C, et al. Defining the Relationship Between Compressive Stress and Tissue Trauma During Laparoscopic Surgery Using Human Large Intestine. IEEE J Transl Eng Health Med 2019;7:3300108.
44. Chebil O, Arnoux PJ, Behr M. Mechanical characterization of human gastrocolic ligament until failure. J Appl Biomater Funct Mater 2015;13:e106-15.
45. Umale S, Deck C, Bourdet N, et al. Experimental mechanical characterization of abdominal organs: liver, kidney & spleen. J Mech Behav Biomed Mater 2013;17:22-33.
46. Khan AF, MacDonald MK, Streutker C, et al. Tissue stress from laparoscopic grasper use and bowel injury in humans: establishing intraoperative force boundaries. BMJ Surg Interv Health Technol 2021;3:e000084.
47. Rahimi-Gorji M, Debbaut C, Ghorbaniasl G, et al. Optimization of intraperitoneal aerosolized drug delivery using computational fluid dynamics (CFD) modeling. Sci Rep 2022;12:6305.
48. Höltzcke P, Sautkin I, Clere S, et al. Feasibility of pressurized intra peritoneal aerosol chemotherapy using an ultrasound aerosol generator (usPIPAC). Surg Endosc 2022;36:7848-58.

49. Piao J, Park SJ, Lee H, et al. Ideal Nozzle Position During Pressurized Intraperitoneal Aerosol Chemotherapy in an Ex Vivo Model. Anticancer Res 2021;41:5489-98.
50. de Bree E, Michelakis D, Stamatiou D, et al. Pharmacological principles of intraperitoneal and bidirectional chemotherapy. Pleura Peritoneum 2017;2:47-62.
51. Solass W, Kerb R, Mürdter T, et al. Intraperitoneal chemotherapy of peritoneal carcinomatosis using pressurized aerosol as an alternative to liquid solution: first evidence for efficacy. Ann Surg Oncol 2014;21:553-9.
52. Tan HL, Kim G, Charles CJ, et al. Safety, pharmacokinetics and tissue penetration of PIPAC paclitaxel in a swine model. Eur J Surg Oncol 2021;47:1124-31.
53. Fröhlich E, Loizou GD. Editorial: 3Rs-Strategies for reduction and refinement of animal studies. Front Pharmacol 2023;14:1200965.
54. Hubrecht RC, Carter E. The 3Rs and Humane Experimental Technique: Implementing Change. Animals 2019;9:754.
55. Khosrawipour V, Khosrawipour T, Diaz-Carballo D, et al. Exploring the Spatial Drug Distribution Pattern of Pressurized Intraperitoneal Aerosol Chemotherapy (PIPAC). Ann Surg Oncol 2016;23:1220-4.
56. Khosrawipour V, Mikolajczyk A, Schubert J, et al. Pressurized Intra-peritoneal Aerosol Chemotherapy (PIPAC) via Endoscopical Microcatheter System. Anticancer Res 2018;38:3447-52.
57. Khosrawipour V, Khosrawipour T, Kern AJ, et al. Distribution pattern and penetration depth of doxorubicin after pressurized intraperitoneal aerosol chemotherapy (PIPAC) in a postmortem swine model. J Cancer Res Clin Oncol 2016;142:2275-80.
58. Kakchekeeva T, Demtröder C, Herath NI, et al. In Vivo Feasibility of Electrostatic Precipitation as an Adjunct to Pressurized Intraperitoneal Aerosol Chemotherapy (ePIPAC). Ann Surg Oncol 2016;23:592-8.
59. Min SH, Yoo M, Hwang D, et al. Hyperthermic pressurized intraperitoneal aerosol drug delivery system in a large animal model: a feasibility and safety study. Surg Endosc 2024;38:2062-9.
60. Ceelen WP, Flessner MF. Intraperitoneal therapy for peritoneal tumors: biophysics and clinical evidence. Nat Rev Clin Oncol 2010;7:108-15.

Cite this article as: Li R, Fan Q, Lin X, Chen R, Luo B, Yang Z, Li Y. A novel nebulized drug delivery system based on an innovative high-pressure peristaltic pump availably applied to pressurized intraperitoneal aerosol chemotherapy. J Gastrointest Oncol 2025;16(1):234-248. doi: 10.21037/jgo-2024-1009

